

Probing quark orbital angular momentum at EIC and EicC

Shohini Bhattacharya,¹ Duxin Zheng,² and Jian Zhou³

¹*RIKEN BNL Research Center, Brookhaven National Laboratory, Upton, NY 11973, USA*

²*Shandong Institute of Advanced Technology, Jinan, Shandong, 250100, China*

³*School of Physics and Key Laboratory of Particle Physics and Particle Irradiation (MOE), Shandong University, QingDao, Shandong, 266237, China*

We propose to extract quark orbital angular momentum (OAM) through exclusive π^0 production in electron-(longitudinally-polarized) proton collisions. Our analysis demonstrates that the $\sin 2\phi$ azimuthal angular correlation between the transverse momentum of the scattered electron and the recoil proton serves as a sensitive probe of quark OAM. Additionally, we present a numerical estimate of the asymmetry associated with this correlation for the kinematics accessible at EIC and EicC. This study aims to pave the way for the first measurement of quark OAM in relation to the Jaffe-Manohar spin sum rule.

1. Introduction—The exploration of nucleon spin structure, sparked by the revelation of the “spin crisis”, has developed into a captivating research field over the past three decades. A central goal of this field is to comprehend the nucleon’s spin in terms of contributions from its underlying partons. Significant progress has been made in deciphering this partonic content of nucleon spin, particularly in constraining contributions from quark and gluon spins in the moderate and large x regions through measurements of parton helicity distributions at accelerator facilities worldwide [1–4]. The upcoming Electron-Ion Collider in the US and China (EIC and EicC) [5, 6] is expected to play a crucial role in precisely determining the gluon helicity distribution at small x . While parton helicities represent a significant fraction of nucleon spin, there remains ample opportunity to investigate the contribution of parton orbital angular momentum to nucleon spin, constituting another key objective of the EIC and EicC.

The kinematic orbital angular momentum (OAM) of quarks and gluons is determined by subtracting their helicity contributions from the total angular momentum contributions, which can be accessed through hard exclusive processes [7, 8]. However, extracting Jaffe-Manohar type parton OAM [9], or equivalently canonical OAM, in high-energy scattering processes poses a significant experimental challenge. Progress in this direction was limited until a connection between parton OAM and Wigner distribution functions [10], or equivalently, Generalized Transverse Momentum-dependent Distributions (GTMDs) [11], was revealed about a decade ago. For the quark case, this connection is given by [12–14],

$$L^q(x, \xi) = - \int d^2 k_{\perp} \frac{k_{\perp}^2}{M^2} F_{1,4}^q(x, k_{\perp}, \xi, \Delta_{\perp} = 0). \quad (1)$$

The quark OAM can be reconstructed by integrating over the x -dependent OAM distribution: $L_q = \int_0^1 dx L_q(x, \xi = 0)$. This relation, coupled with Eq. (1), thus opens a new avenue to directly access the parton canonical OAM contribution to the nucleon spin through GTMDs. In recent years, theoretical efforts have primarily cen-

tered on investigating the experimental signals of the gluon GTMD $F_{1,4}$ [15–19]. In particular, polarization-dependent diffractive di-jet production has been extensively studied in this context. Conversely, the exclusive double Drell-Yan process, the sole known process providing access to quark GTMDs, offers sensitivity to quark GTMD $F_{1,4}$ only in the ERL region [20]. This poses a challenge when extrapolating the distribution to the forward limit; see below in Eq. (1).

In this paper, we introduce a novel observable to experimentally detect the quark GTMD $F_{1,4}$ in the DGLAP region, establishing a direct link to quark OAM through Eq. (1) and overcoming the difficulty discussed above in the context of double Drell-Yan. Our proposal involves the exclusive π^0 production process in electron-proton collisions, $ep \rightarrow e'p'\pi^0$, with a longitudinally polarized proton target. Our analysis demonstrates that the longitudinal single target-spin asymmetry results in a $\sin 2(\phi_{l_{\perp}} - \phi_{\Delta_{\perp}})$ azimuthal angular correlation, where $\phi_{l_{\perp}}$ and Δ_{\perp} denote the azimuthal angles of the transverse momentum of the scattered electron and the recoil proton. This correlation exhibits a direct sensitivity to quark OAM.

The proposed observable stands out as an ideal probe for quark OAM from both theoretical and practical perspectives. Firstly, the background for this process remains clean, free from contamination by final-state soft gluon radiation effects [21–26]. Additionally, our observable, akin to the unpolarized cross section, constitutes a twist-3 contribution. This characteristic enables the maximal enhancement of the asymmetry without being washed out by the unpolarized cross section. We will present numerical results for our observable in EIC and EicC kinematics, showcasing its potential as a promising tool for directly probing quark OAM.

2. Probing the quark GTMD $F_{1,4}$ in exclusive π^0 production—First, let us define the kinematics of the process under consideration,

$$e(l) + p(p, \lambda) \longrightarrow \pi^0(l_{\pi}) + e(l') + p(p', \lambda'). \quad (2)$$

The standard kinematic variables are defined as follows: $Q^2 = -q^2 = -(l-l')^2$, representing the photon's virtuality; and the incoming electron's momentum is parameterized as $l^\mu = (l^+, l^-, l_\perp) = (\frac{Q(1-y)}{\sqrt{2y}}, \frac{Q}{\sqrt{2y}}, \frac{Q\sqrt{1-y}}{y})$. Here, $y = p \cdot q / p \cdot l$ represents the usual momentum fraction. The $\gamma^* p$ center-of-mass energy is given by $W^2 = (p+q)^2$. The pion mass in our calculation is neglected ($l_\pi^2 \approx 0$), simplifying the analysis. We work in the symmetric frame where the initial state and the final state proton carry the transverse momenta $p_\perp = -\Delta_\perp/2$ and $p'_\perp = \Delta_\perp/2$, respectively. The skewness variable is given by $\xi = (p^+ - p'^+)/ (p^+ + p'^+) = -\Delta^+ / (2P^+) = x_B / (2 - x_B)$, where '+' stands for the light-cone plus component and $x_B = Q^2 / 2p \cdot q$, and the momentum transfer squared can be expressed as $t = (p - p')^2 = -\frac{4\xi^2 M^2 + \Delta_\perp^2}{1 - \xi^2}$, with M being the proton mass.

In the near forward region, specifically when $\Delta_\perp \sim 0$, the exclusive π^0 production process receives its leading power contribution from the helicity flip Generalized Parton Distribution (GPD) for a transversely polarized target, as detailed in Ref. [27]. However, in the scenario of an unpolarized or longitudinally polarized nucleon target, the leading power contribution emerges at the twist-3 level. Crucially, the absence of the unpolarized cross section as the leading contribution is pivotal in making the investigated longitudinal-spin asymmetry, which shares a twist-3 nature with the unpolarized cross section, a non-power-suppressed observable. This characteristic positions it as an ideal tool for probing the quark OAM. In the region where the momentum transfer t is exceedingly small, the exclusive π^0 production process becomes susceptible to being dominated by the Primakoff process [28–34]. This dominance arises due to the electromagnetic interaction scaling inversely with t , while the hadronic reaction plateaus as t approaches zero. The $\sin 2\phi$ azimuthal asymmetry, precisely mirroring what we observe in this study, emerges from the interference between the Primakoff process and the contribution from the gluon GTMD $F_{1,4}$, as demonstrated in Ref. [35]. Note also that the linear polarization of the exchanged photon plays an essential role in generating asymmetries through such an interference channel [36, 37]. In this work, we specifically concentrate on the valence quark region, where $\xi \sim 0.1$, thereby permitting the neglect of contributions from both the Primakoff process and the gluon-initiated process [35].

We will perform the calculation within the framework of collinear higher-twist expansion. In the twist analysis, the hard factor $H(k_\perp, \Delta_\perp)$ is expanded in terms of k_\perp/Q and Δ_\perp/Q , where k_\perp denotes the relative transverse momentum carried by the exchanged quarks,

$$H(k_\perp, \Delta_\perp) = H(k_\perp = 0, \Delta_\perp = 0) + \frac{\partial H(k_\perp, \Delta_\perp = 0)}{\partial k_\perp^\mu} \Big|_{k_\perp=0} k_\perp^\mu + \frac{\partial H(k_\perp = 0, \Delta_\perp)}{\partial \Delta_\perp^\mu} \Big|_{\Delta_\perp=0} \Delta_\perp^\mu + \dots \quad (3)$$

The zeroth-order expansion of k_\perp and Δ_\perp yields a null result for both the spin-averaged cross section and the longitudinal polarization-dependent cross section. Following this expansion, the subsequent step involves integrating over k_\perp . Consequently, the scattering amplitudes are expressed as the convolution of the next-to-leading power of Eq. (3) with the GPDs or the first k_\perp -moment of certain GTMDs, including the k_\perp -moment of the quark GTMD $F_{1,4}$ —in other words, the quark OAM distribution.

Before discussing the calculation details, let us briefly recapitulate the definition of the leading twist quark GTMDs for nucleons. GTMDs parameterize the off-forward transverse momentum dependent quark-quark correlator [11, 38],

$$W_{\lambda, \lambda'}^{[\Gamma]} = \int \frac{d^3 z}{2(2\pi)^3} e^{ik \cdot z} \langle p', \lambda' | \bar{q}(-\frac{z}{2}) \Gamma q(\frac{z}{2}) | p, \lambda \rangle \Big|_{z^+=0}, \quad (4)$$

where Γ indicates a generic gamma matrix. The Wilson line in Eq. (4) is suppressed for brevity. Here, we require the parametrization of Eq. (4) in terms of GTMDs for $\Gamma = \gamma^+, \gamma^+ \gamma_5$. In the notation of [11], they are expressed as follows:

$$W_{\lambda, \lambda'}^{[\gamma^+]} = \frac{1}{2M} \bar{u}(p', \lambda') \left[F_{1,1} + \frac{i\sigma^{i+}}{P^+} (k_\perp^i F_{1,2} + \Delta_\perp^i F_{1,3}) + \frac{i\sigma^{ij} k_\perp^i \Delta_\perp^j}{M^2} F_{1,4} \right] u(p, \lambda), \quad (5)$$

$$W_{\lambda, \lambda'}^{[\gamma^+ \gamma_5]} = \frac{1}{2M} \bar{u}(p', \lambda') \left[\frac{-i\varepsilon_\perp^{ij} k_\perp^i \Delta_\perp^j}{M^2} G_{1,1} + \frac{i\sigma^{i+} \gamma_5 k_\perp^i}{P^+} G_{1,2} + \frac{i\sigma^{i+} \gamma_5 \Delta_\perp^i}{P^+} G_{1,3} + i\sigma^{+-} \gamma_5 G_{1,4} \right] u(p, \lambda), \quad (6)$$

where $\varepsilon_\perp^{ij} = \varepsilon^{-+ij}$ with $\varepsilon^{0123} = 1$. The arguments of the GTMDs depend on $(x, \xi, \vec{k}_\perp, \vec{\Delta}_\perp, \vec{k}_\perp \cdot \vec{\Delta}_\perp)$ but have been omitted in the above formulas for the sake of notation convenience. It is interesting to note that, in general, GTMDs are complex-valued functions [11, 39]. In addition to $F_{1,4}$, the quark GTMD $G_{1,1}$ is particularly intriguing. The real part of $G_{1,1}$ encodes information about the quark's spin-orbital angular momentum correlation inside an unpolarized nucleon [11, 12]. These GTMDs have been explored in various models [11, 12, 39–51].

There are a total of four diagrams contributing to the exclusive π^0 production amplitude. Our explicit calculation has confirmed that the contributions from all four diagrams vanish at the leading power. To isolate the twist-3 contribution, we perform an expansion in k_\perp and Δ_\perp . In doing so, it is essential to handle the k_\perp and Δ_\perp dependencies from the exchanged quark legs with utmost care. To address this, we employ a technique known as the special propagator technique, first introduced in Ref. [52]. The inclusion of the special propagator contribution is crucial to ensure electromagnetic gauge invariance. It is noteworthy that an alternative approach,

which also maintains electromagnetic gauge invariance at twist-3 accuracy, has been developed in Refs. [53, 54].

Depending on the various vector structures, the scattering amplitude can be organized into three terms,

$$\begin{aligned}\mathcal{M}_1 &= \frac{g_s^2 e f_\pi (N_c^2 - 1) 2\xi}{2\sqrt{2} N_c^2 \sqrt{1 - \xi^2}} \delta_{\lambda\lambda'} \frac{\epsilon_\perp \times \Delta_\perp}{Q^2} \{ \mathcal{F}_{1,1} + \mathcal{G}_{1,1} \}, \\ \mathcal{M}_2 &= \frac{g_s^2 e f_\pi (N_c^2 - 1) 2\xi}{2\sqrt{2} N_c^2 \sqrt{1 - \xi^2}} \delta_{\lambda, -\lambda'} \frac{M \epsilon_\perp \cdot S_\perp}{Q^2} \{ \mathcal{F}_{1,2} + \mathcal{G}_{1,2} \}, \\ \mathcal{M}_4 &= \frac{i g_s^2 e f_\pi (N_c^2 - 1) 2\xi}{2\sqrt{2} N_c^2 \sqrt{1 - \xi^2}} \lambda \delta_{\lambda\lambda'} \frac{\epsilon_\perp \cdot \Delta_\perp}{Q^2} \{ \mathcal{F}_{1,4} + \mathcal{G}_{1,4} \} \quad (7)\end{aligned}$$

where $f_\pi = 131$ MeV represents the π^0 decay constant, ϵ_\perp denotes the virtual photon's transverse polarization vector, and S_\perp is defined as $S_\perp^\mu = (0^+, 0^-, -i, \lambda)$. $\mathcal{F}_{i,j}$ and $\mathcal{G}_{i,j}$ serve as shorthand notations for complex convolutions involving the GTMDs $F_{i,j}$, $G_{i,j}$, and the π^0 distribution amplitude (DA) $\phi_\pi(z)$. They are expressed as follows,

$$\begin{aligned}\mathcal{F}_{1,1} &= \int_{-1}^1 dx \frac{x^2 \int d^2 k_\perp F_{1,1}^{u+d}(x, \xi, \Delta_\perp, k_\perp)}{(x + \xi - i\epsilon)^2 (x - \xi + i\epsilon)^2} \\ &\quad \times \int_0^1 dz \frac{\phi_\pi(z)(1 + z^2 - z)}{z^2(1 - z)^2}, \quad (8)\end{aligned}$$

$$\begin{aligned}\mathcal{G}_{1,1} &= \int_{-1}^1 dx \int_0^1 dz \frac{\phi_\pi(z)(x^2 + 2x^2z + \xi^2)}{z^2(x + \xi - i\epsilon)^2(x - \xi + i\epsilon)^2} \\ &\quad \times \int d^2 k_\perp \frac{k_\perp^2}{M^2} G_{1,1}^{u+d}(x, \xi, \Delta_\perp, k_\perp), \quad (9)\end{aligned}$$

$$\begin{aligned}\mathcal{F}_{1,2} &= \int_{-1}^1 dx x \frac{\xi(1 - \xi^2) \int d^2 k_\perp k_\perp^2 F_{1,2}^{u+d}(x, \xi, \Delta_\perp, k_\perp)}{M^2(x + \xi - i\epsilon)^2(x - \xi + i\epsilon)^2} \\ &\quad \times \int_0^1 dz \frac{\phi_\pi(z)(1 + z^2 - z)}{z^2(1 - z)^2}, \quad (10)\end{aligned}$$

$$\begin{aligned}\mathcal{G}_{1,2} &= \int_{-1}^1 dx \int_0^1 dz \frac{\phi_\pi(z)(x^2 + 2x^2z + \xi^2)(1 - \xi^2)}{z^2(x + \xi - i\epsilon)^2(x - \xi + i\epsilon)^2} \\ &\quad \times \int d^2 k_\perp \frac{k_\perp^2}{M^2} G_{1,2}^{u+d}(x, \xi, \Delta_\perp, k_\perp), \quad (11)\end{aligned}$$

$$\begin{aligned}\mathcal{F}_{1,4} &= \int_{-1}^1 dx \frac{x\xi \int d^2 k_\perp k_\perp^2 F_{1,4}^{u+d}(x, \xi, \Delta_\perp, k_\perp)}{M^2(x + \xi - i\epsilon)^2(x - \xi + i\epsilon)^2} \\ &\quad \times \int_0^1 dz \frac{\phi_\pi(z)(1 + z^2 - z)}{z^2(1 - z)^2}, \quad (12)\end{aligned}$$

$$\begin{aligned}\mathcal{G}_{1,4} &= \int_{-1}^1 dx \int_0^1 dz \frac{x(4\xi^2z + \xi^2 - 2x^2z + x^2)}{z^2\xi(x + \xi - i\epsilon)^2(x - \xi + i\epsilon)^2} \phi_\pi(z) \\ &\quad \times \int d^2 k_\perp G_{1,4}^{u+d}(x, \xi, \Delta_\perp, k_\perp). \quad (13)\end{aligned}$$

The superscript $u + d$ indicates the summation of up and down quark contributions. For example, $F_{1,1}^{u+d}(x, \xi, \Delta_\perp, k_\perp) = \frac{2}{3} F_{1,1}^u(x, \xi, \Delta_\perp, k_\perp) + \frac{1}{3} F_{1,1}^d(x, \xi, \Delta_\perp, k_\perp)$. Here, z represents the longitudinal momentum fraction of π^0 carried by the quark.

The derivation of the above expressions involves the repeated use of the symmetry property: $\int dz \frac{z \phi_\pi(z)}{z^2(1-z)^2} = \int dz \frac{(1-z) \phi_\pi(z)}{z^2(1-z)^2}$.

A few remarks are now in order. First, we obtain the terms $\mathcal{F}_{1,2}$, $\mathcal{F}_{1,4}$, $\mathcal{G}_{1,1}$, and $\mathcal{G}_{1,2}$ by performing k_\perp expansion, while the Δ_\perp expansion gives rise to the contributions $\mathcal{F}_{1,1}$ and $\mathcal{G}_{1,4}$. Second, the amplitudes \mathcal{M}_1 , \mathcal{M}_2 , and \mathcal{M}_4 exhibit distinct Δ_\perp -dependent behaviors. Notably, \mathcal{M}_2 persists as Δ_\perp approaches zero, even when averaging over S_\perp in the unpolarized cross section. This persistence is attributed to the helicity flip mechanism provided by the quark GTMDs $F_{1,2}$ and $G_{1,2}$, akin to what the gluon GTMD $F_{1,2}$ does [55]. In the forward limit, the GTMD $F_{1,2}$ is related to the Sivers function f_{1T}^\perp [11, 55–57], and the GTMD $G_{1,2}$ reduces to the worm-gear function g_{1T} [11]. The last point to emphasize is that exclusive π^0 production selects a C-odd exchange. This implies that the hard factors associated with $F_{1,1}$, $G_{1,1}$, and $G_{1,2}$ must be even functions of x , while those proportional to $F_{1,2}$, $F_{1,4}$, and $G_{1,4}$ must be odd functions of x . This property is explicitly satisfied by our results.

Assembling all the pieces, we derive the following spin-averaged and single longitudinal polarization-dependent cross section:

$$\begin{aligned}\frac{d\sigma}{dtdQ^2 dx_B d\phi} &= \frac{(N_c^2 - 1)^2 \alpha_{em}^2 \alpha_s^2 f_\pi^2 \xi^3 \Delta_\perp^2}{2N_c^4 (1 - \xi^2) Q^{10} (1 + \xi)} [1 + (1 - y)^2] \\ &\quad \times \left\{ \left[|\mathcal{F}_{1,1} + \mathcal{G}_{1,1}|^2 + |\mathcal{F}_{1,4} + \mathcal{G}_{1,4}|^2 + 2 \frac{M^2}{\Delta_\perp^2} |\mathcal{F}_{1,2} + \mathcal{G}_{1,2}|^2 \right] \right. \\ &\quad \left. + \cos(2\phi) a [-|\mathcal{F}_{1,1} + \mathcal{G}_{1,1}|^2 + |\mathcal{F}_{1,4} + \mathcal{G}_{1,4}|^2] \right. \\ &\quad \left. + \lambda \sin(2\phi) 2a \operatorname{Re} [(i\mathcal{F}_{1,4} + i\mathcal{G}_{1,4})(\mathcal{F}_{1,1}^* + \mathcal{G}_{1,1}^*)] \right\} \quad (14)\end{aligned}$$

where $\phi = \phi_{l_\perp} - \phi_{\Delta_\perp}$ and $a = \frac{2(1-y)}{1+(1-y)^2}$. Eq. (14) stands as the central result of our paper. As demonstrated, the real part of the quark GTMD $F_{1,4}$, and consequently, the quark OAM, leaves a distinct signature through an azimuthal angular correlation of $\sin 2\phi$ in the longitudinal single target-spin asymmetry. Moreover, a $\cos 2\phi$ azimuthal angular modulation in the spin-averaged cross section provides an additional handle onto various components (real and imaginary parts) of the quark GTMDs. Since both unpolarized and polarized cross sections contribute at twist-3, the magnitudes of the asymmetries are not power-suppressed. Consequently, we emphasize that experimentally extracting quark OAM through the $\sin 2\phi$ asymmetry is less challenging compared to, for instance, the azimuthal asymmetry in diffractive di-jet production, which constitutes a power correction.

3. Numerical results—We now present the numerical results for both the unpolarized cross section and the $\sin 2\phi$ asymmetry. It is noteworthy that two of the k_\perp -integrated GTMDs can be linked to the standard unpo-

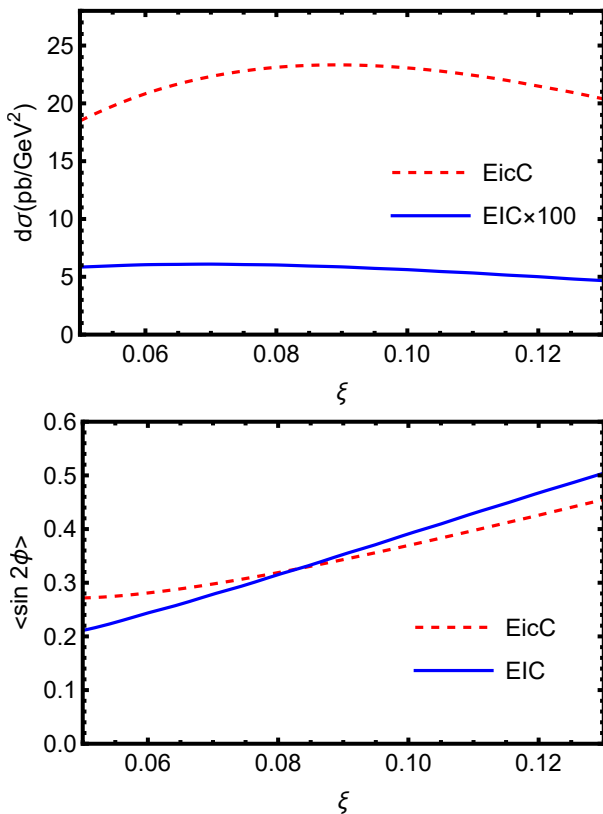


FIG. 1: The unpolarized part of the cross section, as given by Eq. (14), is displayed in the top plot for EIC kinematics with $Q^2 = 10 \text{ GeV}^2$ and $\sqrt{s_{ep}} = 100 \text{ GeV}$, as well as for EicC kinematics with $Q^2 = 3 \text{ GeV}^2$ and $\sqrt{s_{ep}} = 16 \text{ GeV}$. The unpolarized cross section for the EIC case is re-scaled by a factor of 100. The bottom plot shows the average value of $\langle \sin(2\phi) \rangle$ given by Eq. (18) in EIC and EicC kinematics. The variable t is integrated over the range $[-0.5 \text{ GeV}^2, -\frac{4\xi^2 M^2}{1-\xi^2}]$.

larized GPD and the helicity GPD [11],

$$\int d^2 k_{\perp} \text{Re}[F_{1,1}(x, \xi, \Delta_{\perp}, k_{\perp})] \approx H(x, \xi, \Delta_{\perp}), \quad (15)$$

$$\int d^2 k_{\perp} \text{Re}[G_{1,4}(x, \xi, \Delta_{\perp}, k_{\perp})] \approx \tilde{H}(x, \xi, \Delta_{\perp}), \quad (16)$$

where we neglect terms proportional to ξ^2 on the right-hand side of the aforementioned equations. As previously mentioned, the imaginary part of the GTMD $F_{1,2}$ is intricately linked to the quark Sivers function in the forward limit. The Sivers functions for up and down quarks are recognized to exhibit similar magnitudes but with opposite signs. It is reasonable to anticipate that the contributions of $F_{1,2}^u$ and $F_{1,2}^d$ are largely canceled out. The same rationale applies to the $G_{1,2}$ term, which, in the forward limit, is associated with the worm-gear function [58]. Thus, in our first attempt at a numerical study, we choose to neglect contributions from the GTMDs $F_{1,2}$ and $G_{1,2}$, as well as from $G_{1,1}$, which lacks a GPD or TMD counterpart and remains unconstrained

thus far. Regarding the $\mathcal{F}_{1,4}$ and $\mathcal{G}_{1,4}$ terms, we only consider their pole contributions from their imaginary parts. However, for the term $\mathcal{F}_{1,1}$, the magnitude of which is expected to be the largest among all GTMDs, we include both its imaginary and real parts in the numerical estimation.

Note that the hard part becomes divergent as z approaches 0 or 1. This behavior, known as the endpoint singularity, typically signals factorization breaking. From a phenomenological standpoint, regularization is achievable by considering the transverse momentum dependence of the pion DA [59–61]. An effective way to introduce transverse momentum dependence is to modify the upper and lower integration limits of z to $\int_{\langle p_{\perp}^2 \rangle / Q^2}^{1 - \langle p_{\perp}^2 \rangle / Q^2} dz$, where $\langle p_{\perp}^2 \rangle$ is the mean squared transverse momentum of the quark inside the pion, chosen to be $\langle p_{\perp}^2 \rangle = 0.04 \text{ GeV}^2$ [62] in our numerical calculation. For simplicity, we consider the asymptotic form for the pion's DA, $\phi_{\pi}(z) = 6z(1-z)$.

On the other hand, the discontinuity of the derivative of quark GPDs at the endpoints $x = \pm\xi$ (as seen in, for example, Refs. [63, 64]), coupled with the double poles at $x = \pm\xi$, also contributes to a divergent component in the cross section. To resolve this issue, we shift the double pole from $\frac{1}{(x-\xi+i\epsilon)^2}$ to $\frac{1}{(x-\xi-\langle p_{\perp}^2 \rangle / Q^2 + i\epsilon)^2}$ (and similarly for the negative x region) following the same rationale. Essentially, we affirm the necessity of some transverse motion of the partons within the pion and proton to smear the effects of poles at the endpoints and induce a shift.

To provide a model input for the x -dependent quark OAM distribution, specifically the k_{\perp} -moment of $F_{1,4}$, we employ the Wandzura-Wilczek (WW) approximation [65],

$$L_q(x) \approx x \int_x^1 \frac{dx'}{x'} q(x') - x \int_x^1 \frac{dx'}{x'^2} \Delta q(x'), \quad (17)$$

where $q(x')$ and $\Delta q(x')$ denote the usual unpolarized quark PDF and quark helicity distribution, respectively. It is a common practice to reconstruct the ξ -dependence for $L_q(x, \xi)$ from its PDF counterpart $L_q(x)$ using the double distribution method [62, 66, 67]. In this context, we use the JAM (valence) quark PDFs $q(x)$ and $\Delta q(x)$ as inputs in Eq. (17) from Ref. [68]. As for its t -dependence, we adopt a Gaussian form factor, represented by $e^{t/\Lambda}$ with $\Lambda = 0.5 \text{ GeV}^2$. Similarly, we reconstruct the ξ and t -dependence of the GPDs $H(x, \xi, t)$ and $\tilde{H}(x, \xi, t)$ from their PDF counterparts using the double distribution method.

We now present numerical predictions for the EIC and EicC kinematics. The t -integrated unpolarized cross section is shown as a function of ξ in the top panel of Fig. 1. The asymmetry, quantified by the average value of $\sin(2\phi)$ and depicted as a function of ξ in the bottom

plot of Fig. 1, is defined as:

$$\langle \sin(2\phi) \rangle = \frac{\int \frac{d\Delta\sigma}{d\mathcal{P}.S.} \sin(2\phi) d\mathcal{P}.S.}{\int \frac{d\sigma}{d\mathcal{P}.S.} d\mathcal{P}.S.}, \quad (18)$$

where $d\Delta\sigma = \sigma(\lambda = 1) - \sigma(\lambda = -1)$. The unpolarized cross section exhibits a notable magnitude at EicC energy, whereas it is relatively small at EIC energy. Additionally, the asymmetries are substantial for both EIC and EicC kinematics. Examination of the plot suggests an almost linear rise in asymmetries with increasing ξ . Consequently, our numerical results signify that the azimuthal asymmetry $\sin 2\phi$ in exclusive π^0 production stands out as a promising avenue for probing the quark OAM distribution.

4. Summary—We propose extracting the quark OAM associated with the Jaffe-Manohar spin sum rule by measuring the azimuthal angular correlation $\sin 2\phi$ in exclusive π^0 production at EIC and EicC. This observable serves as a clean and sensitive probe of quark OAM for several reasons. Firstly, the azimuthal asymmetry is not a power correction, as both the unpolarized and longitudinal polarization-dependent cross sections contribute at twist-3. Secondly, the produced π^0 transverse momentum $-\Delta_\perp$ remains unaffected by final state QCD radiations. Detecting π^0 makes it less challenging to experimentally measure Δ_\perp , in contrast to the diffractive di-jet production case where reconstructing Δ_\perp from the total transverse momentum of the di-jet system is impossible due to the contamination of final-state soft gluon radiations. Most importantly, this process enables access to the quark GTMD $F_{1,4}$ in the DGLAP region for the first time. In contrast, the exclusive double Drell-Yan process only allows the access of quark GTMD $F_{1,4}$ in the EBRL region, making it challenging to extrapolate the functional form of $F_{1,4}$ to the forward limit.

We computed the differential cross section within the collinear higher-twist expansion framework for both an unpolarized and longitudinally polarized proton target. Despite the substantial uncertainties associated with the model inputs, our numerical results reveal a sizable azimuthal asymmetry, which critically relies on the quark OAM distribution. In the kinematic range accessible to the EIC and EicC, our observable can be thoroughly investigated, paving the way for the first experimental extraction of the canonical quark OAM distribution in the future.

Acknowledgements: The authors would like to express their gratitude to C. Cocuzza for providing the LHAPDF tables of JAM22 PDFs as referenced in [68] and to F. Yuan for insightful discussions. This work has been supported by the National Natural Science Foundation of China under Grant No. 12175118 (J. Z.), and the National Science Foundation under Contract No. PHY-

1516088. S. B. has been supported by the U.S. Department of Energy under Contract No. DE-SC0012704, and also by Laboratory Directed Research and Development (LDRD) funds from Brookhaven Science Associates.

-
- [1] L. Adamczyk et al. (STAR), Phys. Rev. Lett. **115**, 092002 (2015), 1405.5134.
 - [2] D. de Florian, R. Sassot, M. Stratmann, and W. Vogelsang, Phys. Rev. Lett. **113**, 012001 (2014), 1404.4293.
 - [3] E. R. Nocera, R. D. Ball, S. Forte, G. Ridolfi, and J. Rojo (NNPDF), Nucl. Phys. B **887**, 276 (2014), 1406.5539.
 - [4] M. S. Abdallah et al. (STAR), Phys. Rev. D **105**, 092011 (2022), 2110.11020.
 - [5] R. Abdul Khalek et al., Nucl. Phys. A **1026**, 122447 (2022), 2103.05419.
 - [6] D. P. Anderle et al., Front. Phys. (Beijing) **16**, 64701 (2021), 2102.09222.
 - [7] X.-D. Ji, Phys. Rev. Lett. **78**, 610 (1997), hep-ph/9603249.
 - [8] X.-D. Ji, Phys. Rev. D **55**, 7114 (1997), hep-ph/9609381.
 - [9] R. L. Jaffe and A. Manohar, Nucl. Phys. B **337**, 509 (1990).
 - [10] A. V. Belitsky, X.-d. Ji, and F. Yuan, Phys. Rev. D **69**, 074014 (2004), hep-ph/0307383.
 - [11] S. Meissner, A. Metz, and M. Schlegel, JHEP **08**, 056 (2009), 0906.5323.
 - [12] C. Lorce and B. Pasquini, Phys. Rev. D **84**, 014015 (2011), 1106.0139.
 - [13] Y. Hatta, Phys. Lett. B **708**, 186 (2012), 1111.3547.
 - [14] C. Lorce, B. Pasquini, X. Xiong, and F. Yuan, Phys. Rev. D **85**, 114006 (2012), 1111.4827.
 - [15] X. Ji, F. Yuan, and Y. Zhao, Phys. Rev. Lett. **118**, 192004 (2017), 1612.02438.
 - [16] Y. Hatta, Y. Nakagawa, F. Yuan, Y. Zhao, and B. Xiao, Phys. Rev. D **95**, 114032 (2017), 1612.02445.
 - [17] S. Bhattacharya, R. Boussarie, and Y. Hatta, Phys. Rev. Lett. **128**, 182002 (2022), 2201.08709.
 - [18] S. Bhattacharya, A. Metz, V. K. Ojha, J.-Y. Tsai, and J. Zhou, Phys. Lett. B **833**, 137383 (2022), 1802.10550.
 - [19] R. Boussarie, Y. Hatta, B.-W. Xiao, and F. Yuan, Phys. Rev. D **98**, 074015 (2018), 1807.08697.
 - [20] S. Bhattacharya, A. Metz, and J. Zhou, Phys. Lett. B **771**, 396 (2017), [Erratum: Phys.Lett.B 810, 135866 (2020)], 1702.04387.
 - [21] Y. Hatta, B.-W. Xiao, F. Yuan, and J. Zhou, Phys. Rev. D **104**, 054037 (2021), 2106.05307.
 - [22] Y. Hatta, B.-W. Xiao, F. Yuan, and J. Zhou, Phys. Rev. Lett. **126**, 142001 (2021), 2010.10774.
 - [23] C. Zhang, Q.-S. Dai, and D. Y. Shao, JHEP **23**, 002 (2020), 2211.07071.
 - [24] X.-B. Tong, B.-W. Xiao, and Y.-Y. Zhang, Phys. Rev. Lett. **130**, 151902 (2023), 2211.01647.
 - [25] M.-S. Gao, Z.-B. Kang, D. Y. Shao, J. Terry, and C. Zhang, JHEP **10**, 013 (2023), 2306.09317.
 - [26] X.-B. Tong, B.-W. Xiao, and Y.-Y. Zhang (2023), 2310.20662.
 - [27] L. L. Frankfurt, P. V. Pobylitsa, M. V. Polyakov, and M. Strikman, Phys. Rev. D **60**, 014010 (1999), hep-ph/9901429.

- [28] H. Primakoff, *Phys. Rev.* **81**, 899 (1951).
- [29] A. H. Gasparian, *PoS CD15*, 048 (2016).
- [30] G. Liping, R. Miskimen, A. Gasparian, J. Goity, W. Rong, and C. Xurong, *Nucl. Phys. Rev.* **31**, 453 (2014).
- [31] M. M. Kaskulov and U. Mosel, *Phys. Rev. C* **84**, 065206 (2011), 1103.2097.
- [32] G. P. Lepage and S. J. Brodsky, *Phys. Rev. D* **22**, 2157 (1980).
- [33] A. Khodjamirian, *Eur. Phys. J. C* **6**, 477 (1999), hep-ph/9712451.
- [34] Y. Jia, Z. Mo, J. Pan, and J.-Y. Zhang (2022), 2207.14171.
- [35] S. Bhattacharya, D. Zheng, and J. Zhou (2023), 2304.05784.
- [36] C. Li, J. Zhou, and Y.-J. Zhou, *Phys. Rev. D* **101**, 034015 (2020), 1911.00237.
- [37] H. Li and Z. Lu, *Eur. Phys. J. C* **82**, 668 (2022), 2111.03840.
- [38] C. Lorcé and B. Pasquini, *JHEP* **09**, 138 (2013), 1307.4497.
- [39] S. Meissner, A. Metz, M. Schlegel, and K. Goeke, *JHEP* **08**, 038 (2008), 0805.3165.
- [40] K. Kanazawa, C. Lorcé, A. Metz, B. Pasquini, and M. Schlegel, *Phys. Rev. D* **90**, 014028 (2014), 1403.5226.
- [41] A. Mukherjee, S. Nair, and V. K. Ojha, *Phys. Rev. D* **90**, 014024 (2014), 1403.6233.
- [42] Y. Hagiwara, Y. Hatta, and T. Ueda, *Phys. Rev. D* **94**, 094036 (2016), 1609.05773.
- [43] J. Zhou, *Phys. Rev. D* **94**, 114017 (2016), 1611.02397.
- [44] A. Courtoy and A. S. Miramontes, *Phys. Rev. D* **95**, 014027 (2017), 1611.03375.
- [45] D. Boer and C. Setyadi (2023), 2301.07980.
- [46] D. Boer and C. Setyadi, *Phys. Rev. D* **104**, 074006 (2021), 2106.15148.
- [47] Y. Hatta and J. Zhou, *Phys. Rev. Lett.* **129**, 252002 (2022), 2207.03378.
- [48] C. Tan and Z. Lu (2023), 2301.09081.
- [49] S. Xu, C. Mondal, X. Zhao, Y. Li, and J. P. Vary (2022), 2209.08584.
- [50] V. K. Ojha, S. Jana, and T. Maji (2022), 2211.02959.
- [51] V. K. Ojha, S. Jana, and T. Maji (2023), 2309.03917.
- [52] J.-W. Qiu, *Phys. Rev. D* **42**, 30 (1990).
- [53] I. V. Anikin, B. Pire, and O. V. Teryaev, *Phys. Rev. D* **62**, 071501 (2000), hep-ph/0003203.
- [54] A. V. Radyushkin and C. Weiss, *Phys. Rev. D* **63**, 114012 (2001), hep-ph/0010296.
- [55] R. Boussarie, Y. Hatta, L. Szymanowski, and S. Wallon, *Phys. Rev. Lett.* **124**, 172501 (2020), 1912.08182.
- [56] D. Boer, M. G. Echevarria, P. Mulders, and J. Zhou, *Phys. Rev. Lett.* **116**, 122001 (2016), 1511.03485.
- [57] J. Zhou, *Phys. Rev. D* **89**, 074050 (2014), 1308.5912.
- [58] S. Bhattacharya, Z.-B. Kang, A. Metz, G. Penn, and D. Pitonyak, *Phys. Rev. D* **105**, 034007 (2022), 2110.10253.
- [59] S. V. Goloskokov and P. Kroll, *Eur. Phys. J. C* **42**, 281 (2005), hep-ph/0501242.
- [60] S. V. Goloskokov and P. Kroll, *Eur. Phys. J. C* **50**, 829 (2007), hep-ph/0611290.
- [61] P. Sun, X.-B. Tong, and F. Yuan, *Phys. Lett. B* **822**, 136655 (2021), 2103.12047.
- [62] S. V. Goloskokov and P. Kroll, *Eur. Phys. J. C* **53**, 367 (2008), 0708.3569.
- [63] S. Bhattacharya, C. Cocuzza, and A. Metz, *Phys. Lett. B* **788**, 453 (2019), 1808.01437.
- [64] S. Bhattacharya, C. Cocuzza, and A. Metz, *Phys. Rev. D* **102**, 054021 (2020), 1903.05721.
- [65] Y. Hatta and S. Yoshida, *JHEP* **10**, 080 (2012), 1207.5332.
- [66] A. V. Radyushkin, *Phys. Rev. D* **59**, 014030 (1999), hep-ph/9805342.
- [67] A. V. Radyushkin (2000), hep-ph/0101225.
- [68] C. Cocuzza, W. Melnitchouk, A. Metz, and N. Sato (Jefferson Lab Angular Momentum (JAM)), *Phys. Rev. D* **106**, L031502 (2022), 2202.03372.